Vacuum ultraviolet-photoemission study of some sodium tungsten bronzes, Na_xWO_3

R. L. Benbow* and Z. Hurych
Physics Department, Northern Illinois University, DeKalb, Illinois 60115
(Received 22 August 1977)

Synchrotron radiation was the light source for this study. A different view of the valence and conduction bands was provided than that shown by previous x-ray photoemission data. In the present case the *p* angular-momentum character of the electrons is emphasized more than the *d* character. The use of a continuum light source allowed study by photon-energy-dependent spectroscopies. These made possible partial examination of the final states as well as demonstration of the nature of the Na $2p$-core excitations. The latter were found to show excitonic behavior. Effects of a possible Na deleption layer at the surface are discussed.

I. INTRODUCTION

The tungsten bronzes form a set of compounds which have many interesting properties. The most common tungsten bronzes are formed by "dissolving" alkaline metals into a WO_3 matrix, although other metals have been successfully combined with WO_3 to produce similar compounds. The sodium tungsten bronzes were the first to be discovered[1] and are the subject of this paper. Their chemical formula is Na_xWO_3 with $0 \lesssim x \lesssim 1$. For $x \lesssim 0.3$, Na_xWO_3 is a tetragonal semiconductor, but for $x \gtrsim 0.5$, the lattice stabilizes into the perovskite structure,[2] which is incomplete. The W ions occupy the corners of a cube, and the O ions fill in the edges (Fig. 1). The Na ions randomly occupy the centers of the cubes (hence, incomplete), and for $x = 1$, the structure is exactly the perovskite lattice.

Interest in the sodium tungsten bronzes covers a wide range of properties. Some of them are superconductors.[3-5] Their resistivities have been the subject of numerous studies.[6,7] NMR has been performed on them.[8,9] Most of the studies have been aimed at resolving some of the controversy over the nature of the electronic structure of the bronzes.[8-11] Considerable interest in the bronzes arises from their close relation to the transition-metal oxides—particularly to ReO_3.

Historically, it was not clear just what constituted the electronic structure of Na_xWO_3.[8-11] It was known that they were either semiconductors or conductors, depending on x. The first obvious idea was that there should be a Na *s* band. However, NMR studies showed that there were no *s* conduction electrons associated with the Na ions in Na_xWO_3.[8,9] Later, a model was proposed where the conduction electrons were to fall into a Na *p* band.[11] In their review, Dickens and Whittingham[2] point out the strengths and weaknesses of the theory, and compare it to a theory due to Seinco[10] and refined by Goodenough.[12] The latter theory, applied to Na_xWO_3, suggests that the Na atoms give up their 3*s* electrons to partially fill the otherwise empty W 5*d* band, and then the Na ion benignly sits in the center of the cubic cell (Fig. 1). This makes $Na_{1.0}WO_3$ isoelectronic to ReO_3. The approximation is generally accepted for Na_xWO_3 that the number of 5*d* electrons in the conduction band varies linearly with x.

The last point is supported by resistivity measurements,[6,7] optical measurements,[13-16] x-ray photoemission spectroscopy (XPS) data,[17-21] Kohn-effect results,[22] and most recently, by a band-structure calculation.[23] A curious result was obtained in the XPS work. It was thought that XPS should provide a fair representation of the conduction- and valence-band densities of states. In the case of ReO_3,[19] the experimentally derived density of states (DOS) did not agree well with a calculated

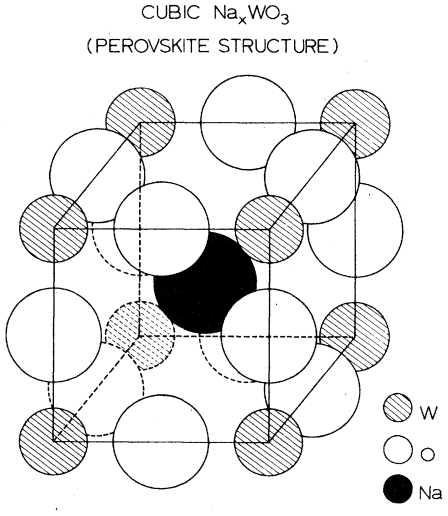

FIG. 1. Perovskite crystal structure. For Na_xWO_3, the oxygen atoms occupy the edges of the cube, the tungsten atoms occupy the corners, and the sodium atoms occupy x of the centers of the cubes.

DOS.[24] It was decided that the XPS data (taken at the Al $K\alpha$ line) showed primarily the residual $5d$ character in the valence band along with the $5d$ conduction band. An explanation is that the partial photoionization cross sections of $5d$ electrons are some 20–40 times larger than for $2p$ electrons.

In the present work, ultraviolet-photoemission-spectroscopy (UPS) studies were made on samples of Na_xWO_3, cleaved *in situ* in ultrahigh vacuum. Tantalus I, the 240-MeV electron storage ring operated by the Synchrotron Radiation Center of the University of Wisconsin—Madison, was the light source for the experiment. The advantages of looking at photoemission from Na_xWO_3 in the range from about 10 to 30 eV are that we can observe effects (if any) of the band-structure or joint DOS regime on the photoemission spectra. Also, partial photoionization cross sections should be different than in the XPS region at the Al $K\alpha$ line, so a different picture of the relative valence- and conduction-band emissions may be possible.

In Sec. II we briefly describe the experiment. The results of the experiment are presented in Sec. III. A discussion of the results as well as the implications of the work are presented in Sec. IV.

II. EXPERIMENTAL

Tunability of the synchrotron continuum was achieved through use of a MacPherson 225 normal-incidence monochromator. A gold-coated spherical concave grating (Bausch and Lomb, 1200 grooves/mm) provided the spectral dispersion in the monochromator. The synchrotron radiation nearly represented a point source, with an actual area of 1 mm^2. A series of grazing-incidence mirrors focused the light at the entrance slit. The diverging light exiting from the monochromator was focused onto the object point of the double-pass cylindrical mirror analyzer (CMA, Physical Electronics Industries, Inc.) by means of a grazing-incidence elliptical mirror. The grating was the only normal-incidence reflecting surface in the optical system. The sample was positioned at the object point of the CMA and arranged such that the angle of incidence was 40° from normal. The angle between the CMA axis and the incident light beam was 75°.

The base pressure in the sample chamber was maintained at about 3×10^{-10} Torr. The samples were cleaved *in situ* by a pair of opposing wedges. Even though the samples were single crystals, the cleaving process usually resulted in a fracture rather than a smooth cleave. Data was taken with the CMA operating in the preretarding mode, with a typical kinetic energy resolution of 0.15–0.4 eV. The photon energies were varied with the monochromator slits set at constant value, so the overall energy resolution in the experiment was also a function of the incident photon energy.

The use of the synchrotron continuum makes possible three modes of photoelectron spectroscopy over a very wide range of photon energy. The first is simply to set the monochromator at a particular photon energy and to scan the energy of the photoelectrons with the CMA. The result is the energy distribution curve (EDC). Several EDC's were obtained at various photon energies in order to examine the photoelectron DOS as a function of photon energy $h\nu$. The second mode is a form of yield spectroscopy. It is a variation of the yield spectroscopy discussed by Gudat and Kunz[25] called the constant-final-state-energy spectroscopy (CFS) by Lapeyre *et al.*[26] It is also referred to as partial photoyield spectroscopy by other workers. In this mode, the acceptance energy of the CMA is held constant while $h\nu$ is scanned. The result is the number of electrons photoemitted into the same kinetic energy window as a function of $h\nu$, i.e., the number of photoelectrons with the same final-state energy. This technique is sensitive to the Auger component of core hole decays, and provides a means of probing the bottom part of the empty conduction band.

The third mode is a bit more complicated. The acceptance energy of the CMA is scanned synchronously with $h\nu$ while maintaining the relation

$$E_f - h\nu = \text{const}. \tag{1}$$

However,

$$E_i + h\nu = E_f, \tag{2a}$$

or

$$E_f - h\nu = E_i. \tag{2b}$$

Thus, by maintaining (1), we are examining photoelectrons which were excited from states with the same initial energy. This form of spectroscopy has been termed constant-initial-state-energy spectroscopy (CIS) by Lapeyre *et al.*[27] The effects of changing the final state relative to various initial states can be more easily observed through the CIS than the EDC's in some cases.

III. RESULTS

Photoemission data were obtained on samples of three different compositions: $x=0.5$, 0.7 and 0.79. As observed in the XPS experiments,[17] only subtle differences were found as a function of x. In the UPS regime, the condition of the surface is extremely important because the photoelectrons originate in the first few atomic layers near the sur-

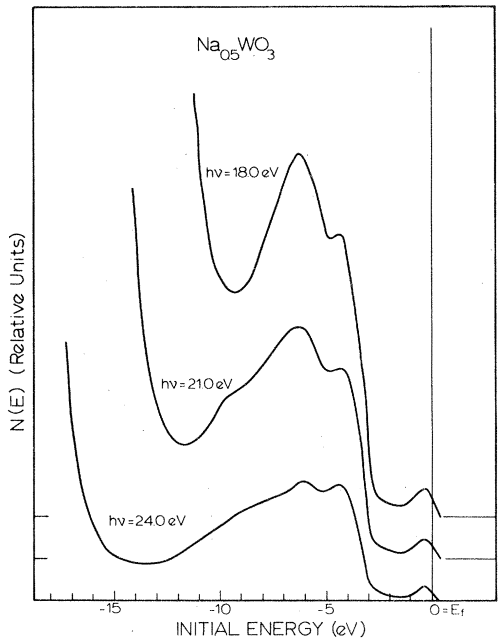

FIG. 2. EDC's for $Na_{0.5}WO_3$ for various photon energies. Only the valence- and conduction-band emissions are shown.

face. Hence, the condition of the surface after a cleave has unmistakable effects upon the spectra obtained.

In Figs. 2 and 3, EDC's of a sample of Na_xWO_3 are shown for $x = 0.5$. There is a small peak near the Fermi energy (E_f) which is due to excitation and emission of conduction electrons. Between about -0.8 and -2.8 eV there is a region of very

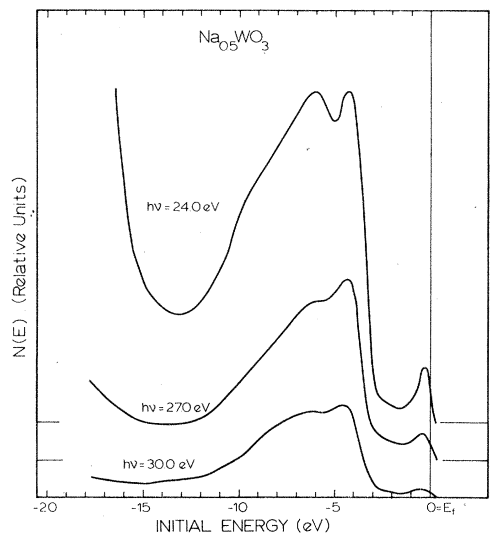

FIG. 3. Continuation of Fig. 2 but with a change of scale.

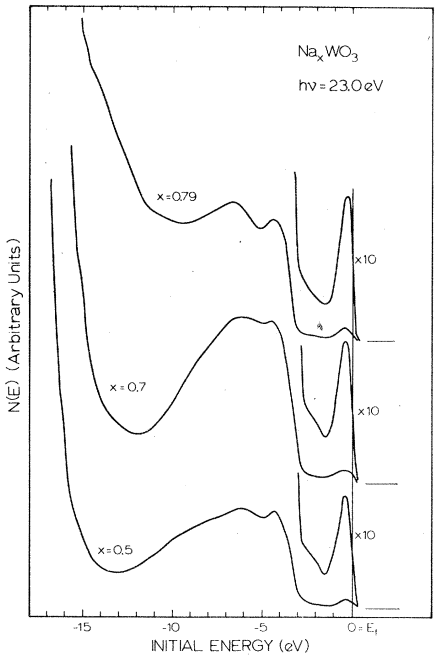

FIG. 4. EDC's for Na_xWO_3 with $h\nu = 23.0$ eV for different values of x. Only the valence- and conduction-band emissions are shown, including an expanded view of the conduction-band DOS.

weak emission. This is the location of the large (~2 eV) energy gap between the bottom of the filled conduction band and the valence band. Two rather strong, broad peaks (at -4.5 and -6.3 eV) characterize emissions from the valence bands. A third feature in the valence region is a shoulder in the photoelectron DOS at -10.0 eV.

EDC's for Na_xWO_3 for different values of x show strong resemblance to one another (Fig. 4). Relative amplitudes of features varied more than the location. Amplitudes varied considerably from cleave to cleave and a consistent variation with x was not observed. The low-energy peak in any EDC (omitted in Figs. 2 and 3) is due to multiply scattered electrons. In the EDC in Fig. 5, the scattered electron peak is the dominant feature, but it is quite narrow and apparently makes a minor contribution to the photoelectron DOS in the valence band region. Such is also the case for $x = 0.5$ and 0.7 in Fig. 4. However, for $x = 0.79$ the low-energy scattered-electron peak is broader and makes a more significant contribution to the emissions from the valence-band region. Interestingly, Chazalviel *et al.*[18] observe a shoulder at ~7 eV higher binding energy than the W 4*f* levels in their XPS data. The shoulder is interpreted as being due to a peak in the joint DOS at about 7 eV, corresponding to peaks in the electron DOS above and below E_F. A peak a few electron volts above E_F in

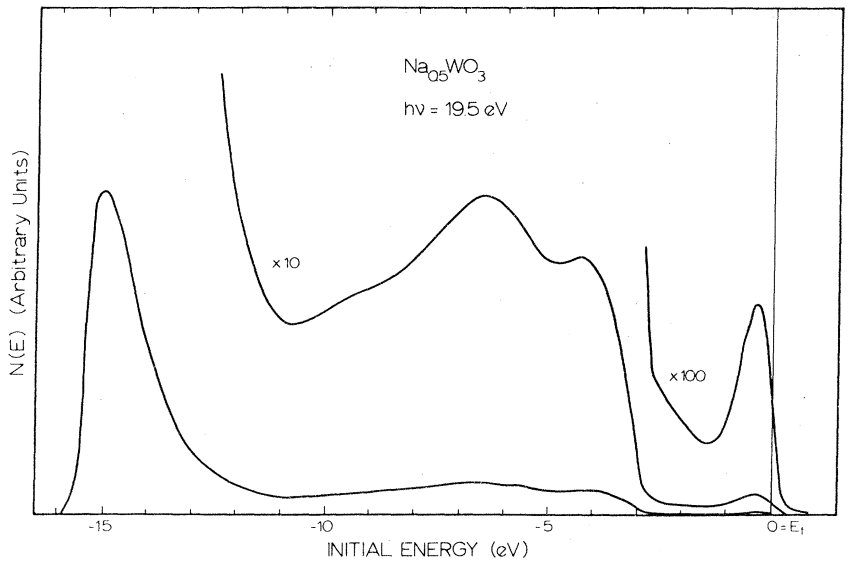

FIG. 5. The complete EDC for $Na_{0.5}WO_3$ with $h\nu = 19.5$ eV. The relative magnitudes of the valence- and conduction-band emissions are compared with the secondary emissions at low energy (on the left).

the electron DOS would affect the shape of the scattered electron peak in an EDC. If additional sharp structures are present in the electron DOS above E_F, the scattered peak could exhibit them, accounting for the structures at $E_i \sim -34$ eV ($h\nu = 40$ eV) on Fig. 6.

Figure 6 shows four EDC's for Na_xWO_3 ($x = 0.79$). For $h\nu = 40$ eV, the complete EDC is shown in segments. The scattered peak has structure, and a core-level emission—the Na $2p$—is observed 30.8 eV below E_F. For this sample, at the higher photon energies, what was a shoulder at -10.0 eV for $x = 0.5$ is now a peak at -9.6 eV. The relative amplitudes of the peak in the photoelectron DOS are seen to vary with photon energy, especially the peak at -4.5 eV.

The amplitude variation of peak heights as well as slight energy shifts when $h\nu$ changes is due to variations in the density of final states accessible at different $h\nu$'s, as well as the transition probability between the initial and final states. To get more definite ideas on the final-state structure, it is advantageous to use the CIS technique. CIS's for two samples are shown in Figs. 7 and 8. The CIS's are multiplied by $E_f^{3/2}$ to attempt to cancel the effect of the escape depth[28] which varies as $E_f^{-3/2}$.

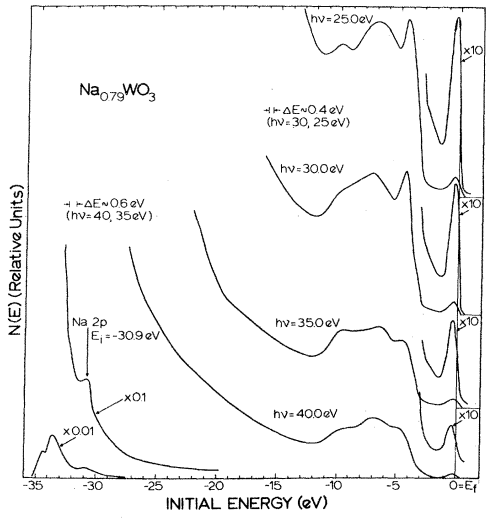

FIG. 6. Series of EDC's for $Na_{0.79}WO_3$ at various photon energies. For $h\nu = 40$ eV, the complete EDC is shown in segments to demonstrate the visibility of the Na $2p$-core emission.

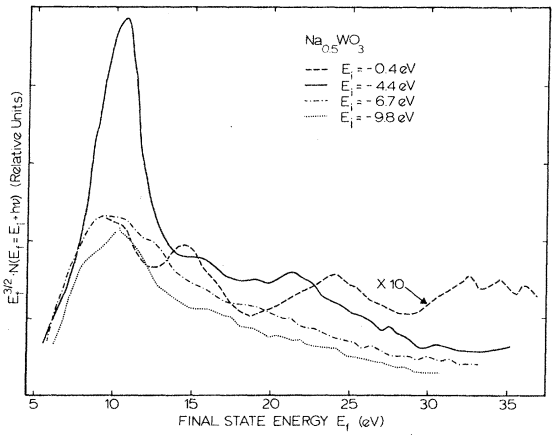

FIG. 7. CIS's for $Na_{0.5}WO_3$ plotted as a function of the final-state energy above the Fermi energy. The factor $E_f^{3/2}$ is included in an attempt to compensate for the attenuation caused by the decreasing escape depth as the energy increases. Because of the weakness of the conduction-band emission, it is shown times 10.

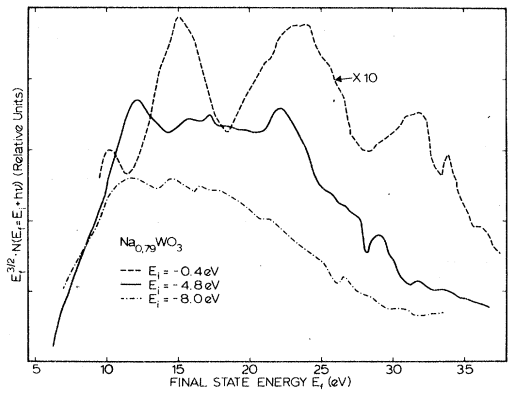

FIG. 8. CIS's for $Na_{0.79}WO_3$ with similar considerations as in Fig. 7.

Of much interest is the CIS for $x=0.79$ and E_i -0.4 eV. It shows broad peaks at $E_f \simeq 15$, 23.5, and 31.5 eV. Similar features are found in the corresponding CIS for $x=0.5$, except that the peaks are not emphasized as much. For the CIS's associated with the structures in the EDC's near the top of the valence band, structures are also present, but are not quite the same as for the previously mentioned CIS's. Specifically, for $x=0.5$, $E_i=-4.4$ eV, there is a strong peak at $E_f=10.5$ eV, and weaker peaks above 15 and 21 eV. For x $=0.79$, $E_i=-4.8$ eV, there are well-defined peaks at $E_f=12$ and 22 eV, and weaker structures at 16–17 eV. There is further a peak at about 22–24 eV in the two CIS's. The remaining CIS's have small peaks and shoulders superposed on a background which has a broad maximum at the lower final-state energies. This maximum (as well as features near 10 eV) is due as much as anything to the increasing contribution of scattered electrons at the low final-state energies.

Since we observe the direct emission of a core state in Fig. 6, we note that we may employ the CFS technique. CFS's for kinetic energy $E_K=5.0$, $x=0.5$ and $E_K=4.0$, $x=0.7$ are presented in Fig. 9. For $x=0.79$, CFS's are shown in Fig. 10 for E_K $=4.0$, 6.0, and 8.0 eV. All five spectra contain three common features: (i) a peak near $h\nu=33.0$ eV; (ii) a peak near 34.5 eV; and (iii) a broad feature with structure which begins just above $h\nu=40$ eV. This last structure is partially obscured by a direct emission from the Na $2p$ core states. There are other structures present, but none replicate themselves in all five CIS's.

IV. DISCUSSION

The analysis of the results can be divided into three main categories: (i) comparison of the estimates valence-band and conduction band DOS to

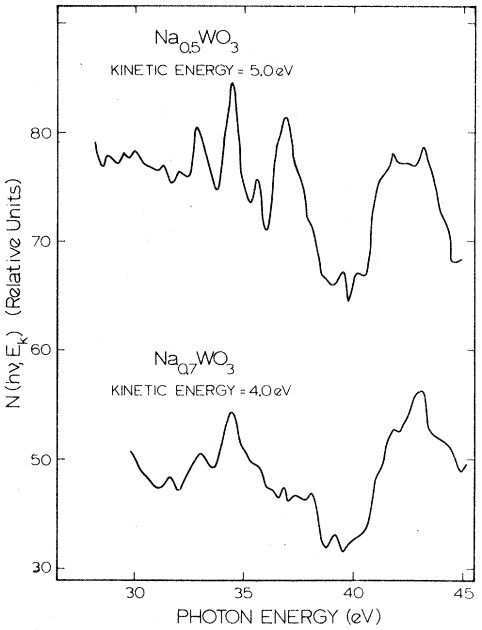

FIG. 9. CFS's for Na_xWO_3 for $x=0.5$ and 0.7. The actual final-state energy is the sum of the kinetic energy and the work function, about 9.1 eV for $x=0.5$ and 8.1 eV for $x=0.7$.

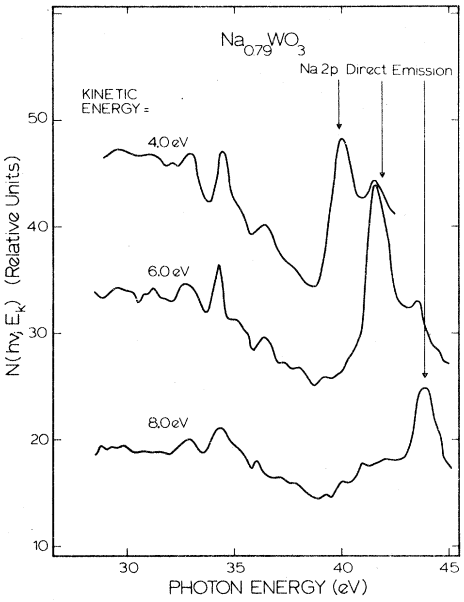

FIG. 10. CFS's for $Na_{0.79}WO_3$ for three kinetic energies corresponding to final-state energies of 8.1, 10.1, and 12.1 eV. The Na-$2p$ direct emissions are shown and the change in location as a function of kinetic energy is demonstrated. Note that the core decay features (at $h\nu$ $=33.0$ and 34.5 eV and possibly at $h\nu=31$ eV) are basically unaffected by a shift in the kinetic energy.

previous work and band-structure calculations; (ii) estimation of the nature of higher-lying bands; and (iii) discussion of the core-level excitations.

A. Valence- and conduction-band emissions

In the past, due to the absence of specific calculations for Na_xWO_3, analysis of optical data[13,14] has been done on the basis of band-structure calculations[24] for ReO_3 while assuming a rigid band model for adapting the ReO_3 bands to Na_xWO_3. XPS data[17,18] have also been discussed by that means as well as by application of a model, due to Wolfram,[29] of the density of states of d-band perovskites, to Na_xWO_3. Recent appearance of a band structure for the tungsten bronzes[23] gives us the opportunity to use that calculation in the analysis of the present results. The band structure of Kopp *et al.*[23] was presented for cubic $NaWO_3$ and cubic WO_3. There is a striking similarity for the two extremes of composition in the valence and conduction bands. The most significant differences come in some of the higher-lying bands where the presence of Na causes distortions and shifts to a greater extent than in the bonding and conduction bands. The most useful result of a band structure for our purposes is the DOS calculation and a decomposition of the DOS into orbital angular-momentum components arising from the different atomic sites.

In Fig. 11 we show the density of states calculated by Kopp *et al.*[23] along with the valence- and conduction-band portion of an EDC where an attempt was made to subtract the scattered background. We have adjusted the Fermi level (solid line) of the calculation so that the gap appears to be in the correct place. Arranged this way, the gap calculated by Kopp *et al.*[23] is very nearly the correct value. Since their Fermi level was established for $x=1$, it is reasonable that the adjusted Fermi energy should be considerably lower. The two peaks in the valence-band data coincide nicely with the two major regions in the calculated DOS, but the experimentally derived density of valence states is much broader.

In Fig. 12 an expanded plot of the conduction-band emissions is shown, along with the top of the valence region. There is a finite emission from the band gap, and it has some structure. This emission is an energy-loss satellite for the conduction electrons. The plasma energy for these compounds is of the order of 2 eV, so one need not be surprised to find electrons emitted from the band-gap region. An attempt is made in Fig. 12 to subtract a background emission from the conduction-band emission and the result is shown above the raw curve. The leftover peak is clearly asymmetrical and the full width at half-maximum is expected to be a measure of the width of the filled conduction band. A typical value for the bandwidth is 0.85 ± 0.10 eV. The point Y in Fig. 12 is the ex-

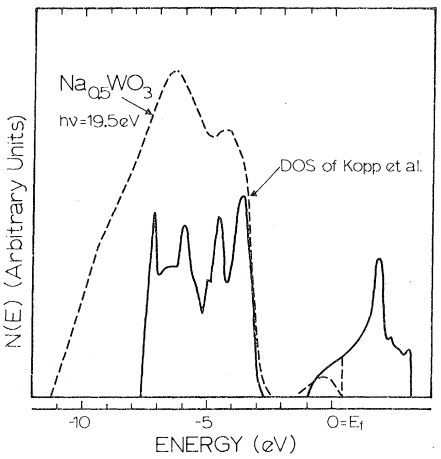

FIG. 11. Comparison of the calculated DOS with an experimentally derived photoelectron DOS covering the valence and conduction bands. An attempt was made to subtract scattered electrons from the experimental data. No sharp features are seen in the experimental data because of scattering of electrons and smoothing due to the instrumental resolution.

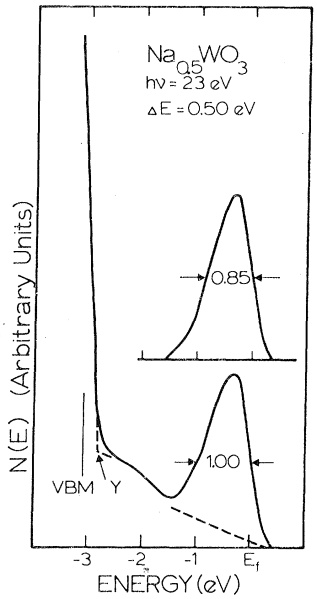

FIG. 12. Demonstration of how the widths of the conduction band and the band gap were estimated. A guess of the shape of the energy-loss satellite was made and then the satellite was subtracted. The result is shown above the raw data. The line marked VBM is 0.25 eV (one-half the instrumental resolution) below the point Y which was taken as the apparent VBM.

perimental valence-band maximum (VBM) after correction for a tiny "tail" (similar to that found at the Fermi level). It is proposed that the acceptable value for the VBM is found by subtracting one-half of the instrumental resolution from Y. The band gap is taken as the separation between Y and the lower half-maximum point in the corrected conduction-band DOS. A typical value for the band gap defined this way is 2.2 ± 0.1 eV. This becomes more reasonable if attention is paid to the width of the down slope in the EDC's at the VBM. The tail-off of emissions is much wider than the instrumental resolution, so the VBM is not simply found at half of the height of the valence emission peak or shoulder near the VBM.

We are not really able to make a good estimate of the width of the valence band, since the likelihood that an energy-loss satellite is making major contributions to emissions in that region precludes finding the bottom of the valence band. One could speculate that the shoulder or (in some cases) peak near -10 eV in the EDC's is due entirely to energy-loss features and that the calculation of Kopp *et al.*[23] is approximately correct, or one could say that the calculation underestimates the bandwidth and the features near -10 eV are genuine band-structure features. Chazalviel *et al.*[18] used the model due to Wolfram[29] to compute the width of the valence band as well as the band gap and the conduction-band DOS. The model of Wolfram[29] appears to give a wider valence band than the calculation of Kopp *et al.*[23] The band-structure calculations of Matthiess[24] for ReO_3 also indicate that the valence band should be somewhat wider since Na_xWO_3 is similar to ReO_3.

B. Final-state effects

The EDC's discussed in the Sec. IV A tend to emphasize the contribution of the initial states to the photoelectron DOS, since any primary structure can be attributed to filled electron states. Observation of changes in the primary structures over a large number of photon energies may show how final states modulate the emissions from a given initial state. A superior way of following this modulation is to observe the photoemission from a particular initial state continuously as a function of $h\nu$. The CIS technique accomplishes the feat of allowing observation from a constant-initial-state energy window as a function of $h\nu$, which is as good as we can hope to do in an integrated photoemission experiment.

There are many things affecting the photoemission of electrons from a solid. One of the things is transport to the surface, step two under the three-step model of photoemission.[30] An electron cannot be photoemitted unless it reaches the surface. Electrons lying farther than one mean scattering length from the surface will likely be inelastically scattered before reaching the surface. In the final-state energy range involved here, the mean scattering length varies approximately as $E_f^{-3/2}$. In Figs. 7 and 8, we have multiplied the measured spectra by $E_f^{3/2}$ in order to offset the escape-depth effect.

Other modulations of the emission from a given initial state include the effect of final states which enter the transition probability through the matrix elements. The final states are Bloch functions arising from the available atomic states of the atoms constituting the lattice and are of the most interest here. There is another possibility, however, for a competing modulation process, excitation to the Bloch functions arising from continuum atomic states. These excitations occur in the vacuum ultraviolet and soft x-ray regions of the electromagnetic spectrum, and in the solid, are usually discussed for core electrons. It may be valid to speak in terms of a photoionization cross section for the conduction and valence electrons as well, since ordinary Bloch final states might not be adequate to define the total emission from the conduction and valence states.

Figures 7 and 8 show the emission spectra for several initial-state energies corresponding to the conduction electrons ($E_i = -0.4$ eV) and valence electrons. The conduction-band spectra have been scaled up by a factor of 10 to make them comparable to the rest. There appear to be three regions of enhanced emission from the conduction bands, at $E_f = 15$, 23.5, and 31.5 eV, with modulations continuing out to higher E_f. These may represent transitions from W $5d$ states to W $6p$ or $5f$ states, or more properly, from bands derived from the states mentioned. If there are continuum effects present, it is difficult to say which effects are due to continuum transitions since there seems to be definite modulation due to other final states. For these conduction-band structures, the peaks at 15 and 23.5 eV could represent W $5d \rightarrow 5f$ or ϵf transitions. In Au, these transitions are known to begin at E_f around 16 (see Ref. 31) to 20 eV (see Ref. 32) above E_F.[33] Later, we shall make a comment on the origin of the structures at $E_f \sim 31.5$ eV.

The CIS's for the peaks near the valence-band maximum ($E_i = -4.4$ eV, $x = 0.5$ and $E_i = -4.8$ eV, $x = 0.79$) show broad maxima centered between final energies of 10 and 20 eV. There are peaks in both curves near $E_f \sim 11$–12, 21–22, and 27–28 eV. These do not correspond in final-state energy with any of the structures observed in the conduction-band CIS's. One is inclined to suggest that these structures are likely to arise from oxygen-derived

final states. The broad maximum between 10 and 20 eV in either curve could be due to transitions to continuum d states. Assume that we can make a valid comparison between the O $2p$ subshell (filled through covalent bonding) and the Ne $2p$ subshell. The photoionization cross section for the latter for transitions to continuum d states peaks just around 12–15 eV above threshold.[34] The broad maxima observed in our spectra are due to the atomiclike transitions from the O $2p$ subshell. The same may be said of all remaining CIS's with E_i deeper in the valence band. For these, there is little consistent structure other than the broad maximum which appears in all the spectra. The atomiclike transitions are dominant in the photon-energy region in this experiment.

In summary, the final-state modulation for the conduction-band states is quite different from that for the valence-band states. The former are regulated by normal crystalline effects, while the latter appear to be dominated by atomiclike behavior.

C. Core-level excitations

The EDC for $h\nu = 40$ eV in Fig. 6 showed the Na-$2p$ direct emission. It is desirable to correlate some of the structure in the CFS's in Figs. 9 and 10 above $h\nu = 31$ eV with Na-$2p$ excitations. In all five CFS's there is a peak near 33 eV and a peak near 34.5 eV which occur independently of the Na concentration or kinetic energy. It appears that there is a weak peak at about $h\nu = 31.3 \pm 0.3$ eV in most of the spectra. Unfortunately, these spectra are taken with a low signal-to-noise ratio, due to reduced flux out of the normal-incidence monochromator in this photon-energy range. There are structures between 35 and 40 eV but these do not occur consistently and are difficult to line up in a recurring fashion.

The binding energy relative to E_F of the Na-$2p$ core states is 30.9 eV for $x = 0.79$ (cf. 31.1 eV in Ref. 17), so this is the energy at which excitations to the empty conduction band should have a threshold. The calculation of Kopp *et al.*[23] shows that there are virtually no Na-derived conduction-band states. It is noteworthy to point out that the peaks at 33 and 34.5 eV are reminiscent of the sharp core-excitonic doublet near 33 eV and the following peak near 34.5 eV in the absorption spectra of the sodium halides[35] or the yield spectra of NaCl at several retarding voltages.[36] The conclusion was reached in Ref. 36 that the peaks represented a core excitonic series. What we probably are observing here is a series of core-exciton-enhanced emissions, but one in which the beginning of the series is broadened by a strong interaction with the conduction-band electrons of only slightly different energy. This leads to an alternative explanation of the enhanced conduction-band emission found near 32 eV in Sec. IV B. The broad peak above 32 eV found in the CIS's with $E_i = -0.4$ eV could be due to conduction electrons excited (and subsequently photoemitted) as a result of the recombinative decay of Na $2p$-core excitons. What we observe in the CFS's are not the usual Auger electrons associated with core-hole decay, but conduction electrons excited when the core-hole–electron pair underwent recombinative decay, and subsequently scattered to lower energy. The extra structures in the CIS's for $E_i = -0.4$ eV in Figs. 7 and 8 above 32 eV may be due to the individual excitonic decays. The more usual Auger mechanism is inhibited by the paucity of Na valence states.[23] The Auger decay would have to be an interatomic process—not very likely because of the small overlap of W and O states with Na states. The excitons can probably exist in these compounds because of the ionic nature of the Na in the crystal. The core-hole–electron interaction is sufficient to keep the electron from becoming itinerant. Lapeyre *et al.*[26] earlier observed the direct recombination of core excitons in KI via the CIS technique.

As mentioned above, the broad increase in emission above 40 eV in the CFS's could be a result of Na $2p \rightarrow \epsilon d$ transitions followed by an Auger decay of the core hole. However, one cannot rule out the possibility of the structure above 40 eV being due to the excitation of the W-$5p_{3/2}$ core level. Since we are restricted by our optical system to photon energies not greater than 40–45 eV, depending on which mode of photoelectron spectroscopy is being used, we are unable to see a direct emission of the W-$5p$ core states although the W-$5p_{3/2}$ core has a binding energy of ~39.2 eV.[18] Excitation of the W-$5p$ core states is a likely event above threshold as absorption spectra on W show.[37] We thus can only state that the increase in photoyield above 40 eV is due to two competing core level excitations.

D. x-dependent properties

Up to this point we have made little mention of any x-dependent properties. There was as much variation in x-dependent properties from samples having the same x as there was from samples with different x's. The most sensitive property we could use to gauge the actual x dependence was the Na $2p$ core emission, which is weak. The emission from the conduction band, which should be linear in x,[17,18] was disappointingly weak and unyielding of consistent information about the width and height of the photoelectron DOS. This may be due to the reduced photoexcitation cross section of

the conduction electrons and the low signal-to-noise ratio for the peak in most of our data. The same limitations apply to experimental determination of the band gap and the work function, since both are determined by the location and shape of the conduction-band emissions. Under the band calculation of Kopp *et al.*[23] the band gap is expected to vary only slightly.

Alternatively, it is possible that the creation of a surface results in a gradient of Na atom concentration normal to the surface. Even if such a gradient extended only a few atomic layers into the sample, the UPS data would be severely affected. Photoelectrons have their origin within one mean scattering length of the surface. For this experiment, the final energy of the electron inside the crystal is typically 15 eV and greater. The escape depth varies as $E^{-3/2}$ and is probably of the order of 10 Å or less—a few atomic layers. Conversely, Na 2*p* direct emissions occur after excitation to final energies of 10 eV or less, where the escape depth is probably greater than 20 Å. Whether such a concentration gradient exists is only partially known.[38] Depth profiles have been taken which show that bulk properties extend very close to the surface, but extensive detail has yet to be obtained about the Na concentration in the 10 or so angstroms closest to the surface.[38] Our indication is that there is a mild depletion near the surface, although our evidence is admittedly circumstantial.[39]

V. CONCLUSIONS

UPS has been performed on several samples of Na_xWO_3 for various values of x. Indications are that a mild depletion of Na near the surface affects the photoelectron DOS for the conduction bands, but actual documentation of such a depletion is lacking. Aside from x-dependent features such as width of the conduction band and of the band gap, x-independent features which are functions of the photon energy have been studied. These include the valence-band DOS, final-state effects for both valence and conduction bands, and the nature of excitations of the Na-2*p* core states and their effects upon the valence- and conduction-band emissions.

The widths of the conduction band and band gap agree quite well with the band-structure calculation to the extent that the two quantities may be determined. The optical coupling of the conduction electrons to the available final states is different from the coupling of the valence-band electrons to the same final states. This may contain information regarding the atomic states from which some of the higher-lying bands originated. The width of the valence bands was not determined experimentally because of probable interference from energy-loss satellites in the photoelectron spectra.

The excitations of the Na 2*p* core states seem to be typical of excitations of the same states in other compounds, notably NaCl. Rather than making transitions to any conduction-band states, the 2*p* core is excited into excitonic states. The decay of the excitonic series is observed in the CFS's, and direct recombination of the excitons is indicated by increased conduction-band emission above final-state energies of 32 eV.

VI. ACKNOWLEDGMENTS

Appreciation is extended to the staff of the University of Wisconsin Synchrotron Radiation Center (supported by NSF Contract No. DMR-74-15089) for making experimentation at the storage ring both convenient and pleasant. In particular, gratitude is extended to Ednor M. Rowe and Roger A. Otte for their fine cooperation during the tenure of this work. Howard Shanks of the Ames Laboratory of the ERDA (at Iowa State University) graciously provided the samples for the experiment. Our work was supported by NSF Contract No. DMR-76-16436.

*Mailing address: Synchrotron Radiation Center, University of Wisconsin, 3725 Schneider Drive, Stoughton, Wisc. 53589.

[1]F. Wöhler, Ann. Phys. (Leipzig) 2, 345 (1824).
[2]P. G. Dickens and M. S. Whittingham, Q. Rev. Chem. Soc. 22, 30 (1968).
[3]C. J. Raub, A. R. Sweedler, M. A. Jensen, S. Broadsten, and B. T. Matthias, Phys. Rev. Lett. 13, 746 (1964).
[4]H. R. Shanks, Solid State Commun. 15, 753 (1974).
[5]K. L. Ngai and R. Silberglitt, Phys. Rev. B 13, 1032 (1976).
[6]H. R. Shanks, P. H. Sidles, and G. C. Danielson, Adv. Chem. Ser. 39, 237 (1963).
[7]L. D. Ellerbeck, H. R. Shanks, P. H. Sidles, and G. C. Danielson, J. Chem. Phys. 35, 298 (1961).
[8]A. Narath and D. C. Wallace, Phys. Rev. 127, 724 (1962).
[9]A. T. Fromhold, Jr. and A. Narath, Phys. Rev. 136, A487 (1964).
[10]M. J. Sienko, J. Am. Chem. Soc. 81, 5556 (1959).
[11]A. R. Mackintosh, J. Chem. Phys. 38, 1991 (1963).
[12]J. B. Goodenough, Czech. J. Phys. B 17, 304 (1967) and references therein.
[13]D. W. Lynch, R. Rosei, J. H. Weaver, and C. G. Olson, J. Solid State Chem. 8, 242 (1973).
[14]J. H. Weaver and D. W. Lynch, Phys. Rev. B 6, 3620 (1972).

[15]J. Feinleib, W. J. Scouler, and A. Ferretti, Phys. Rev. 165, 765 (1968).
[16]P. Camagni, A. Manara, G. Campagnoli, A. Gustinetti, and A. Stella, Phys. Rev. B 15, 4623 (1977).
[17]M. Campagna, G. K. Wertheim, H. R. Shanks, F. Zumsteg, and E. Banks, Phys. Rev. Lett. 34, 738 (1975).
[18]J.-N. Chazalviel, M. Campagna, G. K. Wertheim, and H. R. Shanks, Phys. Rev. B 16, 697 (1977).
[19]G. K. Wertheim, L. F. Mattheiss, M. Campagna, and T. P. Pearsall, Phys. Rev. Lett. 32, 997 (1974).
[20]B. A. DeAngelis and M. Schiavello, Chem. Phys. Lett. 38, 155 (1976).
[21]G. K. Wertheim, M. Campagna, J.-N. Chazalviel, and H. R. Shanks, Chem. Phys. Lett. 44, 50 (1976).
[22]W. A. Kamitakahara, B. N. Harmon, J. G. Taylor, L. Kopp, H. R. Shanks, and J. Rath, Phys. Rev. Lett. 36, 1393 (1976).
[23]L. Kopp, B. N. Harmon, and S. H. Liu, Solid State Commun. 22, 677 (1977).
[24]L. F. Mattheiss, Phys. Rev. 181, 987 (1969); Phys. Rev. B 2, 3918 (1970).
[25]W. Gudat and C. Kunz, Phys. Rev. Lett. 29, 169 (1972).
[26]G. J. Lapeyre, A. D. Baer, J. Hermanson, J. Anderson, J. A. Knapp, and P. L. Gobby, Solid State Commun. 15, 1601 (1974).
[27]G. J. Lapeyre and J. Anderson, Phys. Rev. Lett. 35, 117 (1975).
[28]The escape depth for electrons is proportional to the mean scattering length in the solid and this varies as $E^{-3/2}$; see, for example R. L. Benbow and Z. Hurych, Phys. Lett. A 60, 253 (1977).
[29]T. Wolfram, Phys. Rev. Lett. 29, 1383 (1972).
[30]C. N. Berglund and W. E. Spicer, Phys. Rev. 136, A1030 (1964).
[31]C. G. Olson, M. Piacentini, and D. W. Lynch, Phys. Rev. Lett. 33, 644 (1974).
[32]J. Hermanson, J. Anderson, and G. Lapeyre, Phys. Rev. B 12, 5410 (1975).
[33]The authors of Ref. 31 used the bands of Connolly and Johnson [J. W. D. Connolly and K. H. Johnson, Massachusetts Institute of Technology Solid State and Molecular Theory Group Report No. 72, 1970 (unpublished), p. 19]. The work in Ref. 32 was interpreted in terms of the bands of Christensen and B. O. Seraphin, Phys. Rev. B 4, 3321 (1971).
[34]David J. Kennedy and Steven Trent Manson, Phys. Rev. A 5, 227 (1972).
[35]R. Haensel, C. Kunz, T. Susaki, and B. Sonntag, Phys. Rev. Lett. 20, 1436 (1968).
[36]R. Haensel, G. Keitel, G. Peters, P. Schreiber, B. Sonntag, and C. Kunz, Phys. Rev. Lett. 23, 530 (1969).
[37]J. H. Weaver and C. G. Olson, Phys. Rev. B 14, 3251 (1976).
[38]H. R. Shanks (private communication).
[39]In footnote number 22 of Ref. 17, a discussion of the effects of a concentration gradient near the surface are discussed. In the XPS data, such a gradient would alter line shapes in much the same manner as would many-body effects.